

## UNITED STATES AIR FORCE RESEARCH LABORATORY

### DESIGNING HUMAN-MACHINE INTERFACES USING PRINCIPLES OF STOCHASTIC RESONANCE

Daniel W. Repperger

HUMAN EFFECTIVENESS DIRECTORATE  
CREW SYSTEM INTERFACE DIVISION  
WRIGHT-PATTERSON AFB OH 45433-7022

C. A. Phillips

WRIGHT STATE UNIVERSITY  
DEPARTMENT OF BIOMEDICAL  
AND HUMAN FACTORS ENGINEERING  
3640 COLONEL GLENN HIGHWAY  
DAYTON OH 45435-0001

James E. Berlin

SYTRONICS, INC.  
4433 DAYTON XENIA ROAD  
DAYTON OH 45432

A. Neidhard

WRIGHT STATE UNIVERSITY  
DEPARTMENT OF BIOMEDICAL  
AND HUMAN FACTORS ENGINEERING  
3640 COLONEL GLENN HIGHWAY  
DAYTON OH 45435-0001

Michael W. Haas

HUMAN EFFECTIVENESS DIRECTORATE  
CREW SYSTEM INTERFACE DIVISION  
WRIGHT-PATTERSON AFB OH 45433-7022

APRIL 2001

INTERIM REPORT FOR THE PERIOD SEPTEMBER 1999 TO JANUARY 2001

Approved for public release; distribution is unlimited

Human Effectiveness Directorate  
Crew System Interface Division  
2255 H Street  
Wright-Patterson AFB, OH 45433-7022

20030401 012

## NOTICES

When US Government drawings, specifications, or other data are used for any purpose other than a definitely related Government procurement operation, the Government thereby incurs no responsibility nor any obligation whatsoever, and the fact that the Government may have formulated, furnished, or in any way supplied the said drawings, specifications, or other data, is not to be regarded by implication or otherwise, as in any manner licensing the holder or any other person or corporation, or conveying any rights or permission to manufacture, use, or sell any patented invention that may in any way be related thereto.

Please do not request copies of this report from the Air Force Research Laboratory. Additional copies may be purchased from:

National Technical Information Service  
5285 Port Royal Road  
Springfield, Virginia 22161

Federal Government agencies and their contractors registered with the Defense Technical Information Center should direct requests for copies of this report to:

Defense Technical Information Center  
8725 John J. Kingman Road, Suite 0944  
Ft. Belvoir, Virginia 22060-6218

## TECHNICAL REVIEW AND APPROVAL


AFRL-HE-WP-TR-2002-0187

This report has been reviewed by the Office of Public Affairs (PA) and is releasable to the National Technical Information Service (NTIS). At NTIS, it will be available to the general public.

The voluntary informed consent of the subjects used in this research was obtained as required by Air Force Instruction 40-402.

This technical report has been reviewed and is approved for publication.

**FOR THE COMMANDER**



MARIS M. VIKMANIS  
Chief, Crew System Interface Division  
Air Force Research Laboratory

**REPORT DOCUMENTATION PAGE**Form Approved  
OMB No. 0704-0188

Public reporting burden for this collection of information is estimated to average 1 hour per response, including the time for reviewing instructions, searching existing data sources, gathering and maintaining the data needed, and completing and reviewing the collection of information. Send comments regarding this burden estimate or any other aspect of this collection of information, including suggestions for reducing this burden, to Washington Headquarters Services, Directorate for Information Operations and Reports, 1215 Jefferson Davis Highway, Suite 1204, Arlington, VA 22202-4302, and to the Office of Management and Budget, Paperwork Reduction Project (0704-0188), Washington, DC 20503.

1. AGENCY USE ONLY (Leave blank)

2. REPORT DATE  
APRIL 2001

3. REPORT TYPE AND DATES COVERED

INTERIM REPORT September 1999 to January 2001

4. TITLE AND SUBTITLE

Designing Human-Machine Interfaces Using Principles of Stochastic Resonance

5. FUNDING NUMBERS

PR: 7184

TA: 08

WU: 69

6. AUTHOR(S)

Daniel W. Repperger \*C.A. Phillips \*\* James Berlin  
\* A. Neidhard Michael W. Haas

7. PERFORMING ORGANIZATION NAME(S) AND ADDRESS(ES)

\* Wright State University  
Department of Biomedical  
and Human Factors Engineering  
Dayton OH\*\* Sytronics, Inc  
4433 Dayton-Xenia Road, Building 1  
Dayton OH 45432

8. PERFORMING ORGANIZATION

9. SPONSORING/MONITORING AGENCY NAME(S) AND ADDRESS(ES)

Air Force Research Laboratory  
Human Effectiveness Directorate  
Crew System Interface Division  
Air Force Materiel Command  
Wright-Patterson AFB OH 45433-7022

10. SPONSORING/MONITORING

AFRL-HE-WP-TR-2002-0187

11. SUPPLEMENTARY NOTES

12a. DISTRIBUTION/AVAILABILITY STATEMENT

Approved for public release; distribution is unlimited.

12b. DISTRIBUTION CODE

13. ABSTRACT (Maximum 200 words)

An experimental study is described which involves two types of haptic sensory information and its impact on the ability of the human operator to perform a target tracking task. A principal termed, "stochastic resonance" was applied to design the haptic interface to enhance the operator's sense of presence. In essence, the way that stochastic resonance works, is to provide a sufficiently small amount of noise into a nonlinear system in such a way that the overall system is stimulated, but not degraded in performance. Too little noise or too much noise input is not beneficial to the operator. A small amount of noise, however, presented in a judicious manner can be shown to stimulate the process but not to degrade its efficacy. In this study, haptic (force reflecting joystick) inputs were provided to the operator through his hand as well as haptic (motion chair) inputs as derived by a motion chair in the Human Sensory Feedback Laboratory. The results (across seven subjects) clearly demonstrated that an optimum amount of noise from the haptic joystick and motion chair combination could improve the ability of the operator to track signals and provide higher signal to noise ratios in his response.

14. SUBJECT TERMS

Stochastic Resonance, Design of Human-Machine Interfaces

15. NUMBER OF PAGES  
48

16. PRICE CODE

17. SECURITY CLASSIFICATION  
OF REPORT

Unclassified

18. SECURITY CLASSIFICATION  
OF THIS PAGE

Unclassified

19. SECURITY CLASSIFICATION  
OF ABSTRACT

Unclassified

20. LIMITATION OF  
ABSTRACT

Unlimited

This Page Intentionally Left Blank

# TABLE OF CONTENTS

INTRODUCTION.....	6
Literature Review.....	6
Block Diagram Description.....	8
A Physics Example to Illustrate the SR Effect.....	8
A Threshold Formulation of the SR Effect.....	11
Objectives of SR Study.....	15
Hypothesis of SR Study.....	16
METHOD.....	17
Subjects.....	17
Apparatus – The Motion Based Chair Facility.....	17
The Haptic Stick Controller .....	19
Experimental Design.....	19
The Performance Task (Disturbance Rejection) .....	19
Training.....	20
Data Analysis.....	21
Experiential Scenario.....	23
RESULTS OF THE SR PERFORMANCE STUDY.....	23
DISCUSSION ON THE SR PERFORMANCE RESULTS.....	26
RESULTS FROM THE STICK AND CHAIR ORTHOGONALITY STUDY.....	27
Objective in Studying Orthogonal Stick and Chair Response.....	30
Hypothesis in Studying Orthogonal Stick and Chair Response.....	30
Data Analysis in Stick and Chair Orthogonality Study.....	30
DISCUSSION ON THE STICK AND CHAIR ORTHOGONALITY STUDY.....	33
CONCLUSIONS.....	33
REFERENCES.....	34
Appendix A – Derivation of S/N Ratios for Linear Systems.....	37
Appendix B – Derivation of S/N Ratios for Certain Nonlinear Systems.....	39
Appendix C – The Class of Systems That Exhibit SR.....	46

This Page Intentionally Left Blank

## INTRODUCTION

Conventional thinking has held that when noise or some exogenous disturbance is added to a physical system, generally most performance measures degrade, accordingly. For a linear system, it can be shown (Appendix A) that any addition of noise will degrade the signal/noise ratio as seen at the output in a monotonic manner. Thus noise is not generally viewed as a welcome addition to a working system.

For certain classes of nonlinear systems, however, it will be shown that there are some advantages in adding small amounts of noise in the sense that specific outputs (and the ratio of these outputs to specialized (deterministic) inputs) may be enhanced to some degree. Appendix B presents a mathematical derivation on why such an effect should occur for certain classes of nonlinear systems. Appendix C describes a wide class of nonlinear systems that will benefit from this SR (stochastic resonance) effect. A literature review is first presented on the concept of stochastic resonance to set the stage for the use of this methodology with application in the design of human-machine interface devices.

## LITERATURE REVIEW

Stochastic resonance was first reported in 1981 as an explanation of why the Earth's ice ages have a 100,000-year periodicity, when the correct period should be a factor of ten higher (Benzi et al., 1981). Experimentally, stochastic resonance was initially demonstrated in an electronic circuit known as the Schmitt trigger (Fauve and Heslot, 1983). Stochastic resonance effects have been described in a wide range of physical systems including crayfish (Wiesenfeld and Moss, 1995), neural spike trains and neurons (Richardson et al., 1998, Longtin, 1993, and Svirskis and Rinzel, 2000), in

human tactile sensation (Cordo, et al., 1996, and Collins, et al., 1996a, 1997), in atomic force microscopes (Rajaram et al., 2000, Basso, et al., 1999) and in extended systems (Bulsara and Gammaitoni, 1996). The theory of stochastic resonance describes how the signal to noise ratio of a nonlinear system may be improved by the small insertion of a random signal (McNamara and Weisenfeld, 1989 and Heneghan, et al., 1996). The deterministic input signal (different from the noise input) to the nonlinear system does not have to be strictly periodic (Collins et al., 1995b, 1996b), but such a weak signal can be shown to be amplified by the noise process in the presence of a threshold (Gammaitoni, et al., 1998, and Collins, et al., 1995a). The process of stochastic resonance can be performed adaptively (Yang, et al., 1998), and for multiple systems in parallel (Gailey, et al., 1997). Such effects are shown in physiological systems (Christini and Collins, 1997) since such structures have nonlinear dynamics, which are amenable to this approach (Martin and Schovanec, 1997, and Wilson, 1999). It is interesting to note that as early as 1976, it was reported in the literature that small amounts of dither (noise or a signal orthogonal to an original, deterministic, input signal) into a nonlinear system could enhance its stability as well as improve other performance measures (Zames and Shneydor, 1976). The SR process has now been applied to many dynamically diverse systems, which are too numerous to describe. The goal here is to employ this concept to the design of a human-machine interface in some manner, which is optimal with respect to a selected system response characteristic.

To understand how SR works, it is worthwhile to first formulate and describe the process within the context of a block diagram description.



## Block Diagram Description

With reference to Figure 1, the nonlinear system of interest has two inputs. The first input is  $S(t)$  (deterministic signal) which, for simplicity, is assumed to be a periodic waveform. The stochastic or second input is the noise term  $\xi(t)$ , which is assumed to be a white-gaussian process. The output of the system in Figure 1 is the state vector  $x(t)$  and the goal is to maximize some measure of transfer characteristics ( $x/S$ ) between the output variable  $x(t)$  and the deterministic signal  $S(t)$  input. Typically this transfer characteristic may be the signal to noise ratio, which could be of interest, for example, in a communication's system. To understand why such a methodology would work, a simple physics example clearly shows, in a physical sense, why such a phenomenon has some utility in certain types of natural processes.

### A Physics Example to Illustrate the SR Effect

Figure 2 portrays a configuration that physicists commonly call a bi-potential well problem. The physical relationship of the block diagram of Figure 1 to the system in Figure 2 can be understood by discussing the behavior of the small ball trapped inside the left-most potential well in Figure 2. The input variable  $S(t)$  is the displacement of the ball to the right or left. The output variable is  $x(t)$ , which is the horizontal position of the ball in the well. The ball is initially trapped in the left most well because the signal  $S(t)$  does not have sufficient strength to climb the barrier height  $h$  and move from a State 1 position to a State 2 position. Thus the ball stays in State 1 if the signal  $S(t)$  is of a periodic nature but never has sufficient magnitude to drive the ball to a vertical height in excess of  $h$  units (the height of the potential well). However, if a noise signal is now added to  $S(t)$ , it may be possible for the ball to reach the height  $h$ , go right, pass through the origin, and

move onto State 2 in the diagram. Also if the ball is in State 2 and there was no noise disturbance, then the ball would, again, be trapped in that state forever. With sufficiently large values of noise added to the signal  $S(t)$ , then the ball can move freely between the two states. Without the noise, the ball can never switch states. Too much noise power,

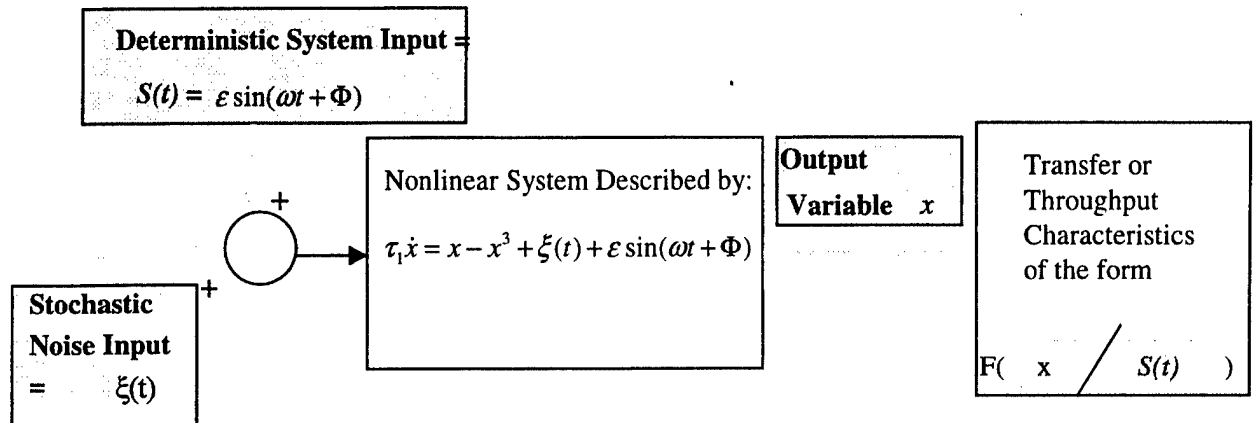


Figure 1 – The Process of Producing Stochastic Resonance

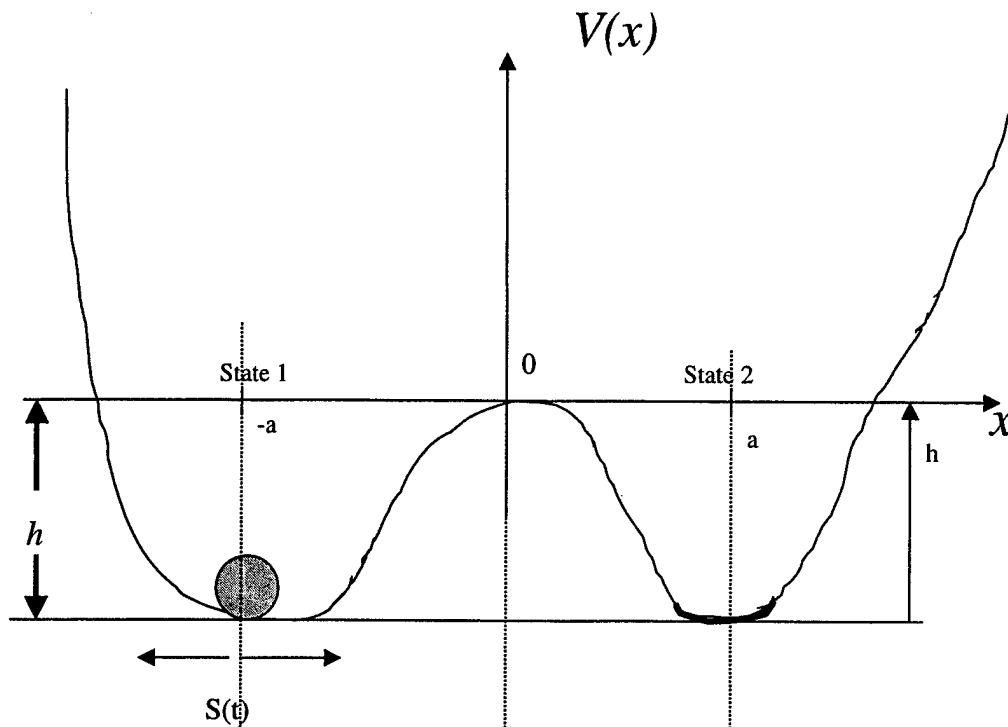


Figure 2 – The Bi-Potential Well Problem

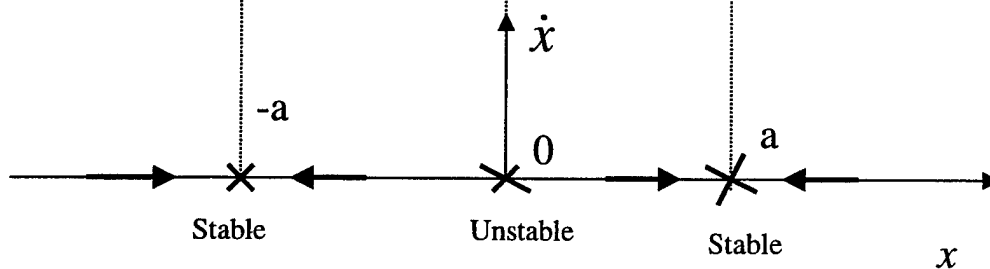


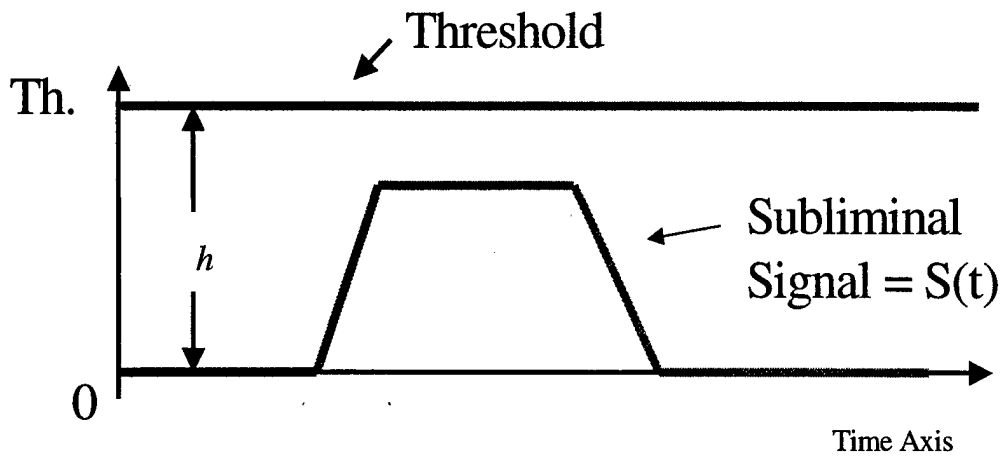
Figure 3 – Equilibrium Points for the Physical System

however, can cause performance degradation. With too high of a noise intensity added to  $S(t)$ , one can see the ball would switch states so frequently that the output of the system ( $x(t)$ ) would appear to represent, mainly, a stochastic disturbance with a noise power

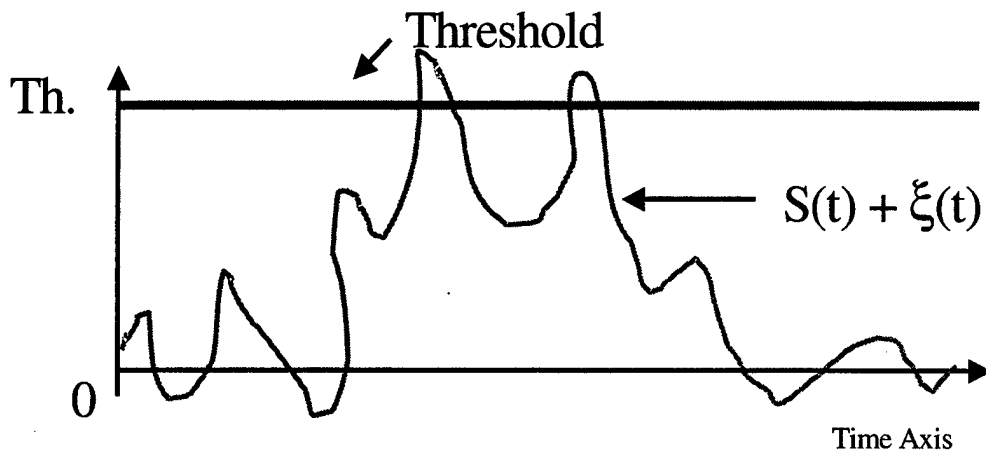
significantly higher than the deterministic signal  $S(t)$ . In this case the noise would mask  $S(t)$ , which is not the desired result. Hence the benefit is reduced when too much noise is added. Figure 3 illustrates equilibrium points for the dynamical system in Figure 2 based on physical considerations. The points denoted as  $\pm a$  are the stable equilibrium points and the origin is classified as an unstable equilibrium point. Obviously the system, when perturbed from the stable equilibrium points ( $\pm a$ ), returns to the original stable state (assuming small perturbations). For the unstable equilibrium point at the origin, however, small perturbations move the ball away from the origin in either direction; hence the origin is at an unstable equilibrium point. A mathematical formulation of the physical system in Figure 2 will be described in the sequel demonstrating additional aspects of the equilibrium points denoted in Figure 3. It will be shown that only a nonlinear system could generate this stochastic resonance effect, but these nonlinear systems occur quite commonly in nature. Hence this design has applicability to a diverse number of physical processes (Appendix C). It is worthwhile to consider an alternative representation of Figures 2-3 in which the signal  $S(t)$  may be alternatively viewed as a subthreshold input which stays less than a threshold value analogous to the height of the potential well, denoted as  $h$  in Figure 2.

### A Threshold Formulation of the Stochastic Resonance Effect

Figure 4 illustrates an alternative means of describing SR within the context of a sub threshold signal. In the top most chart of Figure 4, it is seen that the signal  $S(t)$  is the subliminal signal characterized as the trapezoidal input below the threshold value  $h$ . The objective is to detect the subliminal signal  $S(t)$  when it may be subthreshold. This may be viewed as providing a means of reducing the threshold level  $h$  in Figure 4. The variable  $h$



Now Add a *Little* Noise to the Subliminal Signal



Now Add *a Lot of* Noise to the Subliminal Signal

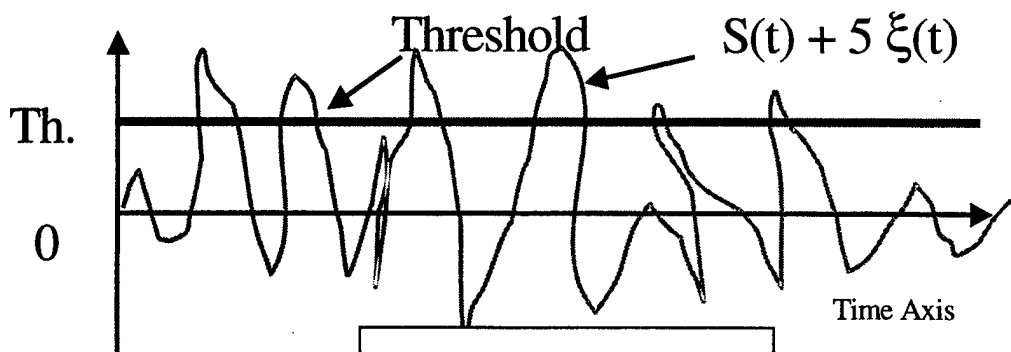


**Figure 4**

in Figure 4 is analogous to the  $h$  in Figure 2. The middle chart in Figure 4 shows what happens when a small amount of random noise is added to the subliminal signal. It is now obvious that when the combined noise and the  $S(t)$  signal are sufficiently high, the subliminal signal now pierces through the threshold and the signal is detected. Thus there has been a reduction of missed negatives to the detection of the threshold signal when  $S(t)$  is high and added to the noise disturbance. The bottom chart of Figure 4 shows the same signal  $S(t)$  now added to a noise source with a high variance (or noise power). Here the signal is correctly detected when  $S(t)$  is high, but it is also mistaken when the original subliminal signal was low. Thus the missed negatives in the detection process are now practically nonexistent, however, the false positives (detecting the signal when it is not high) are increasing. Hence too much noise degrades the decision making process of detecting a subliminal signal by increasing the false positives to the point where they produce incorrect decisions. Figure 5 now combines this description with Figure 4 to show how the resonance actually occurs.

In Figure 5, the top of the diagram is the previous Figure 4. The bottom illustration is a plot (dependent variable) proportional to the probability of detection of the subliminal signal versus the variance or the power in the noise source (independent variable). For the bottom diagram, as the noise is small (in variance, going up the left side of the SR curve), moving to the right, it is observed that the number of missed negatives decreases (for increasing noise power) but the number of false positives starts to increase. A peak point (resonance point) is reached in which the number of missed negatives has significantly decreased (at the expense of including some false positives) so the decision rule is optimal. To the right of this resonance point, the number of false positives keeps increasing but the value gained from reducing any additional missed negatives are not

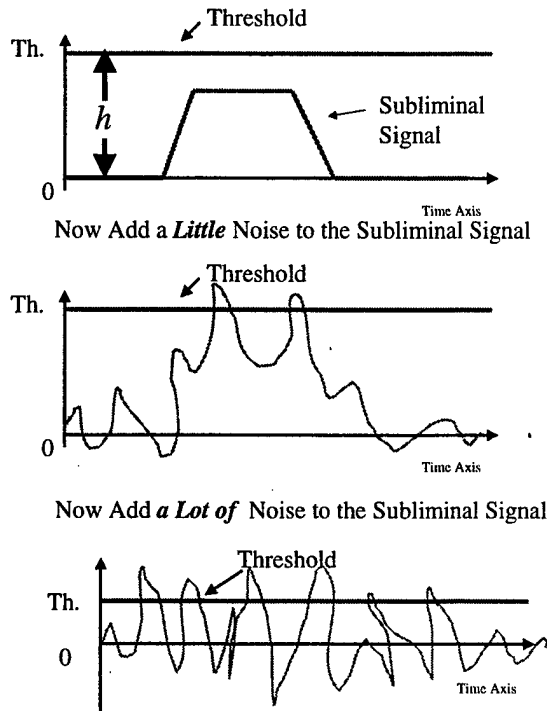
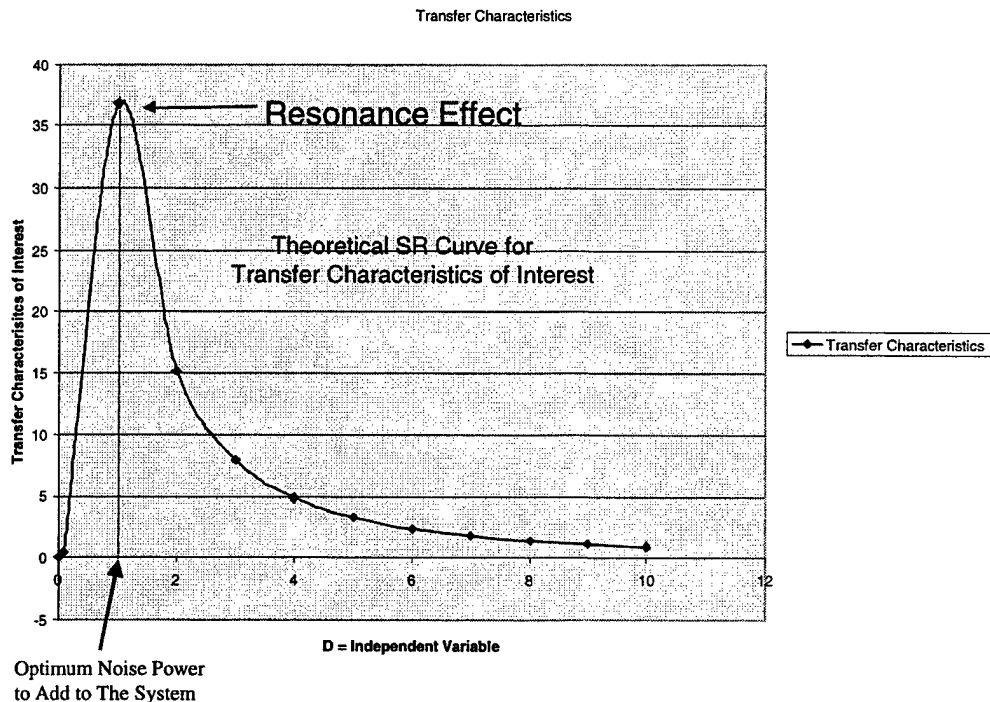


**Figure 5**



of great utility. Consequently the decision rule now suffers as the noise power increases and eventually there is little benefit in the decision process from increasing the noise.

The key point in Figure 5 is that a most favorable point exists where the noise makes the

system an optimal decision maker, much better than the case of having no noise. At this resonant point, the decision maker has minimized his missed negatives at the expense of absorbing a small number of false positives. This is his best operating point because reducing any more missed negatives adds substantially more false positives, thus compromising the overall decision making process. Note that for the no noise situation, since  $S(t)$  is a subliminal signal, all responses are missed negatives. There are no false positives but the decision maker is also not aware of the subliminal signal. Thus, the noise helps the decision maker perform better as compared to the situation of having no noise at all. It is desired to now apply this concept in the design of human-machine interface devices. One can view the human operator as a decision maker who makes errors and is exposed to various types of uncertainties both externally from an exogenous environment as well as internally through faulty measurement and detection processes inherent in the human sensing system. For the human-interface design problem to be described, the role of the noise will be to stimulate and enhance the alternative sensory modality information channels of the operator about the remote tracking task. The goal will be to expand on the ability of the human to perform or make better decisions via improved signal/noise characteristics or transinformation capability.

### Objectives of The SR Study

The intention of this study was to investigate if decision making, which may be manifested by tracking performance improvements, or might be improved as a consequence of noise injection into a multisensory study involving a haptic stick and a motion chair device. The appropriate level of noise injection is of interest as well as any



synergy that may exist between the force reflecting joystick and the motion-based chair system. The tracking task is of a disturbance rejection type representing a flying situation, e.g. a helicopter hovering above a fixed (low) altitude for a search and rescue mission. Typically in such situations, the pilot has to maintain an unvarying altitude and orientation (constant pose) and is subjected to extremely high wind turbulence induced by the presence of the helicopter being so proximal to the ground. This is a disturbance rejection task in the truest sense of the word. The pilot has to maintain a “status quo” set point condition in the presence of external disturbances such as wind turbulence. Thus the pilot has to reject the disturbances to maintain a constant, fixed pose, in space. These objectives can be stated by the following hypothesis.

### Hypothesis of The SR Study

The null hypothesis we wish to reject is that the haptic stick and/or the proprioceptive information provided by the chair motion device provides no performance advantage (using different dependent measures) in this disturbance rejection task. Thus it is desired to reject:

*H<sub>0</sub>*: Either the haptic stick or the motion feedback provided by a laterally translating chair do not influence tracking performance in a disturbance rejection task.

## **METHOD**

### **Subjects**

A total of nine subjects participated in this experiment. A subject panel from a local contractor at the Wright-Patterson Air Force Base in Ohio, USA provided five of the participants. These adult people were either housewives or students at a local university being employed part time. The compensation for participation in this experiment was about \$6 dollars (US) an hour for their participation. The remainder of the subjects were a US Air Force civil servant and contractor personnel.

### **Apparatus-The Motion Based Chair Facility**

This single-axis motion platform was outfitted with a dual axis force reflecting joystick controller (Immersion 2000) as displayed in Figure 6 with the experimental design conditions portrayed in Figure 7. This device was constructed from a welded aluminum frame rigidly supporting a racing car seat. Padded armrests are configured at an elbow level, while the joystick is mounted such that its handle may be comfortably grasped by a seated pilot's right hand. Joystick motion was restricted to the lateral axis, the axis parallel to the motion of the chair. The entire frame translates sideways on a Ball Screw assembly with an 18-inch stroke. Translation is driven by a Kollmorgen Model B-404-B DC Servo Motor, which is rated at 4.5 hp. The motion based chair which resides in the Human Sensory Feedback Laboratory at WPAFB was built to investigate the effects of chair motion and force feedback (via the joystick) on human performance. The bandwidth, range of lateral motion travel, velocities and accelerations are depicted in Table I to describe the capability of this hardware system.

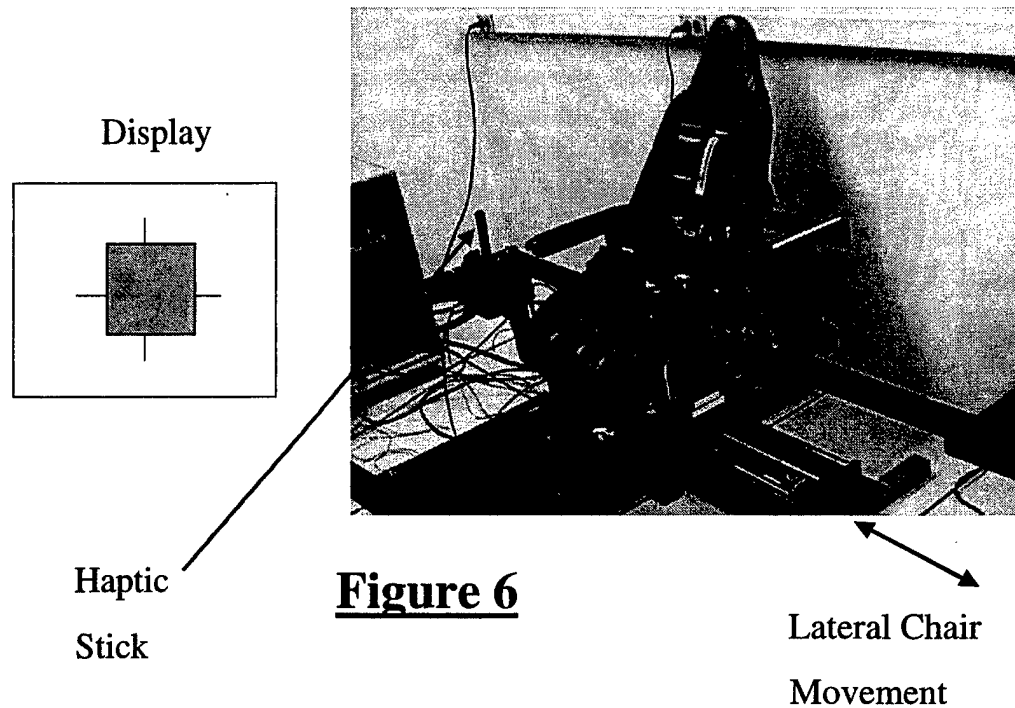


**Figure 6**

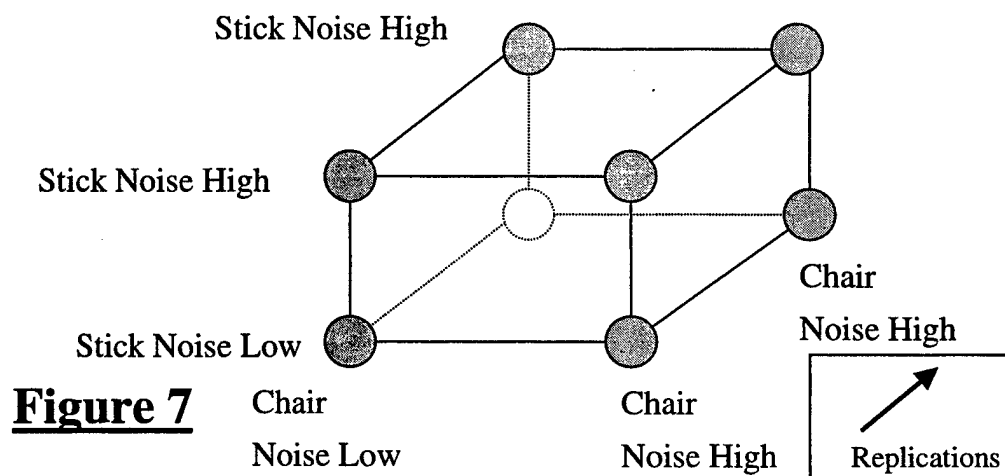


**Figure 7**

Table I – Hardware Specifications of the Motion Chair Device in Figure 6

Performance Parameters ↓	Nominal Case	Worst Case Values
Frequency (Bandwidth of Motion Response of Chair)	3 Hz	4 Hz
Range of Travel	$\pm 5$ cm	$\pm 7.5$ cm
Peak Velocity	1 meter/second	1.8 meters/second
Peak Acceleration	Approximately 2 G	Approximately 4.5 G

### The Haptic Stick Controller

The Immersion IE (Impulse Engine)-2000 powered joystick is a two-degree of freedom force-reflecting manipulandum used in haptic experiments. It generates about 4.04 Newtons maximum force at the handle grip to the human operator, which is displaced 0.1397 meters from a pivot point. This device measures position displacement of the stick through digital encoders and applies a force feedback interface via a cable drive. The force reflection algorithms are programmable in C+ code. The forces generated by this haptic device are independent of the chair's motion but the chair may induce a physical interaction upon the human operator to generate biodynamic feedthrough at the joystick.

### Experimental Design

#### The Performance Task (Disturbance Rejection)

The deterministic input tracking task  $S(t)$  was composed of the sum of 5 distinct sine waves (prime number multiples of a fundamental harmonic) of sufficiently high frequency content that they appeared quasi-random to the human operator. A means of developing such tracking tasks is discussed, for example, in the appendix of Repperger et

al., 1983. It is well known that when 5 or more sine waves are randomly added, it becomes exceedingly difficult for the operator to predict the next movement of the target; hence it has the appearance of a random tracking task, although derived from a deterministic signal. The noise source (for both the stick and the chair motion) originated from a random number generator. The data were sampled at 33.3 Hz (.030 ms). At the start of the run, the random number generator was queried for an initial point within a uniform density function range from zero to one. The extracted number was multiplied by a different initial constant each day which provided the starting point in selecting the noise from a white-noise generator. At each sample point, the white noise element (which could be positive or negative) was then determined and scaled by a display gain before being added to the  $S(t)$  signal. The value of the display gain was established via some pilot studies (increased in magnitude) until at least 50% of the signal was outside the box depicted on the screen in Figure 6. After the pilot study was complete, the same value of display gain was run for all 9 subjects that participated in the experiment.

### Training

On the first day, subjects tracked 5 runs of 2 minutes duration with no chair motion or stick feedback. The second and subsequent days they received the four experimental conditions depicted in Figure 7 after running the baseline condition, initially (the first run was the baseline condition consisting of no noise on the chair motion and no such disturbance on the joystick). The last four runs were randomized each day to mitigate ordering effects and Figure 7 describes the experimental design conducted here. The subjects trained by tracking the disturbance rejection task with the goal of minimizing the error (centering the box of 1.75 inches of width within the domain of a cursor-cross in Figure 6). The cursor-cross consisted of two 4 inch lines commonly

intersecting. The subjects were seated in the motion chair with a distance of about 65 inches from the TV display monitor. Light conditions were dimmed so that the subjects could concentrate on the disturbance rejection task. The subjects tracked five tasks each day until they showed less than 5% variation in their performance scores. Figure 8 illustrates a learning curve for a typical subject. The dependent variable was the time (in seconds) the cursor was outside the domain of the box. The independent variable is the day number, and as can be seen in the diagram, it was not unusual for a subject to perform the experiment for 15 days or more. The last 4 days were considered data collection days.

### Data Analysis

Fifteen channels of data were collected. The most relevant variables include the stick displacement output, chair motion, stick force, target motion as well as the time derivatives of a number of these variables. The analysis reported here included performance (measured by time on target when the box was totally outside the cursor), as well as some additional variables known to be affected when haptics interacts with humans during tracking tasks. The motivation for using haptic manipulandum devices is inspired by the fact that it is known, for example, that the force reflection condition active can mitigate spastic response of individuals (Repperger, et al. 1995). In a landing task study during wind turbulence (Repperger, et al., 1997), haptics, which had a spatial force reflecting condition, were shown to give pilots an additional sense of presence when the visual

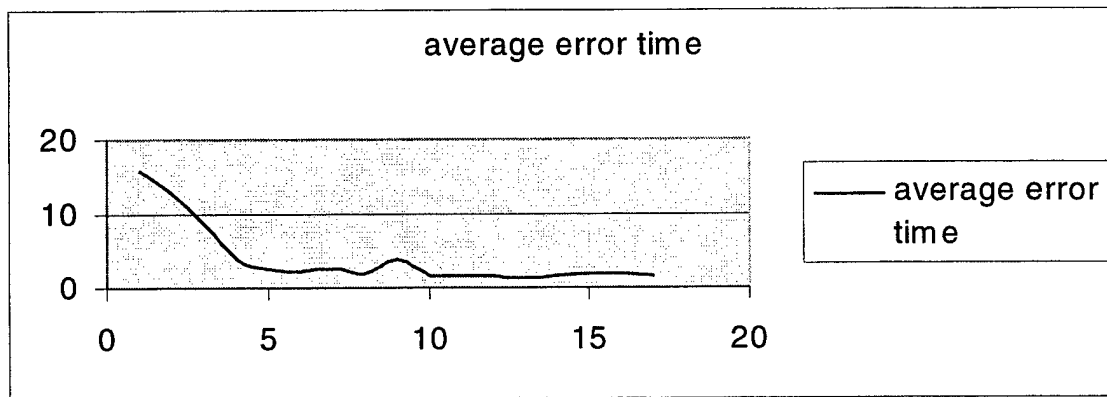


Figure 8 - Typical Learning Data - Time off Target versus Day Number

scene may be compromised (reduced visual field). Another interesting result from the prior haptics studies is that it has been demonstrated that the percent of the stick output correlated with the target task is substantially higher when performance is improved (Repperger, 1991). An issue of interest in this study is whether the haptics improved this “efficiency” of the operator to better process information as manifested by his tracking performance as well as how the stick controller was utilized. A more “efficient” operator may be viewed as having a stick output more highly correlated with the target-tracking task. The prior haptic studies demonstrated that by modulating the force characteristics of the joystick manipulandum, this important correlation variable could be influenced and improved.

## Experimental Scenario

The experimental design was a two variable, full factorial, and repeated measures. This implies each subject was exposed to all treatment conditions (within subject design, hence each subjects acts as his own control). The first independent variable (two levels) was the haptic stick being either low or high (low corresponds to a displacement stick with the addition of a minor level of noise inputted via a force reflected signal). The high condition for the haptic stick represents a much higher level of the force feedback signal related to the exogenous disturbance, which is much like that which would occur in the operational environment. The second independent variable (two levels) was the chair motion (also driven by the noise) being either high or low. Again, the low level of chair motion was barely perceptible. A higher level of chair motion was selected to be no greater than 1.5G maximum lateral acceleration. Several dependent performance measures were considered with the primary metric presented here as the time the box target was sufficiently removed from the origin set point (outside the domain of the cursor-cross) which represented the zero error position. This is very akin to the operational environment, e.g. when a helicopter operator has to maintain a constant pose in a low altitude mission (search and rescue) where the induced wind turbulence creates a significant problem in the control of such an air vehicle.

## RESULTS OF THE SR PERFORMANCE STUDY

The risk level that we incorrectly reject the null hypothesis (when  $H_0$  is true) was selected as  $\alpha = .05$ . This gives a 95% confidence in our decision process. Since this was a within subjects design, blocking across subjects normally occurred which reduced this



source of variation (within a block, however, all other experimental conditions were randomized). We look at the main effects and study their respective interactions.

The main dependent performance measure reported here was the total time the box was outside the domain of the cursor-cross during the 120-second run(cf. Fig. 6). In the real world, this is related to changes in aircraft lateral attitude off a desired set point. In practice, this is representative of a pilot maintaining his aircraft attitude in some desired inertial frame reference position when the aircraft is exposed to external wind turbulence. The data described herein were averaged over the nine subjects that participated including replications of four days for data collection. Figure 9 illustrates plots of the mean values of the time outside the target error from the desired orientation or pose vector (referenced to zero). The five experimental conditions displayed included the baseline data (no noise on either the stick or the chair = C0S0), the low level of noise on the haptic stick but with no chair disturbance = C0S1, low levels of both noise on the haptic stick as well as noise on the chair = C1S1, the case of high stick noise and low chair noise = C1S2, and finally the situation where the stick noise is high and the chair noise was also high = C2S2. In Figure 9, the means of this time off target tracking error are the lower part of the bar graph (averaged across all nine subjects) with the respective standard deviation displayed as the upper part of each bar graph.

Figure 10 illustrates the data for all nine of the trained subjects to show some of the typical variability across subjects but also portrays the consistency across the treatment conditions selected in this experimental design. Thus the improved haptic condition affects individuals differently, but similar trends appear which are reflected in the summary data displayed in Figure 9.

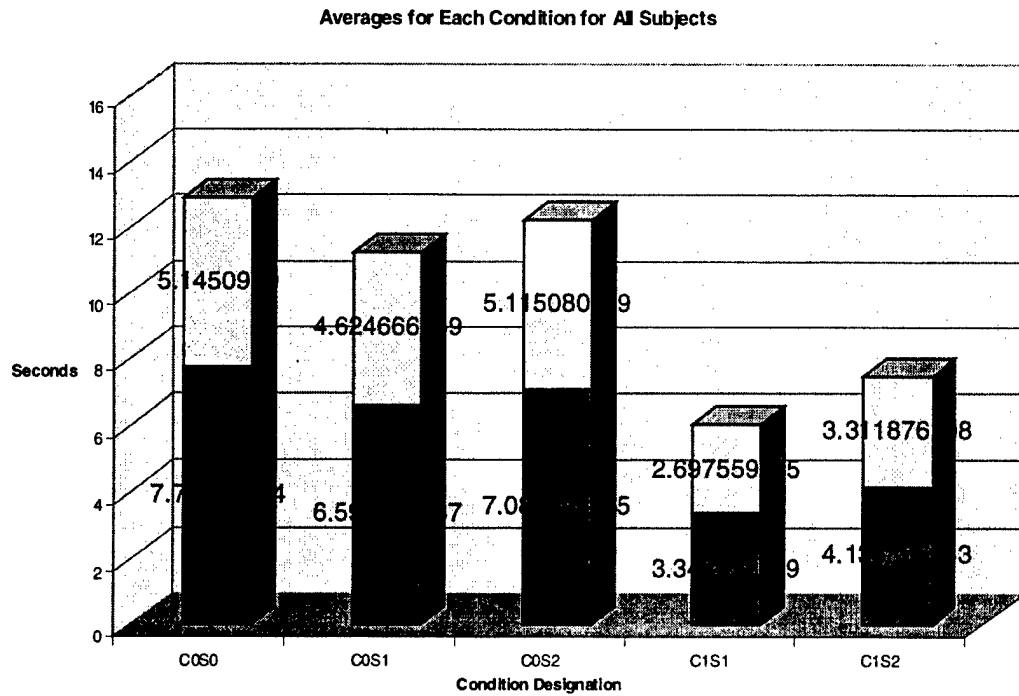


Figure 9 - Averages across nine subjects – Time off Target Tracking Error

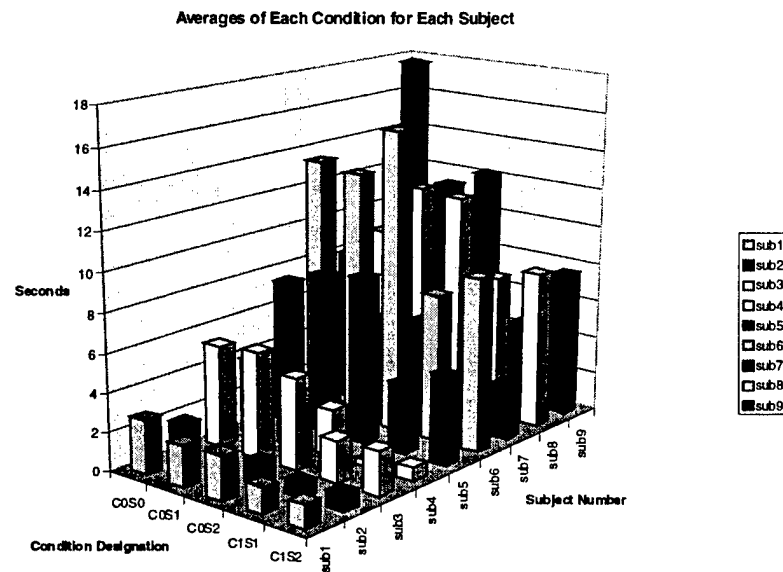


Figure 10 - Results for the Individual Subjects

Using the statistical package, SYSTAT<sup>®</sup> 8.0, Table II illustrates significant effects for the normalized dependent measure-time off target from this ANOVA. In Table II, the p value and F values are given for the dependent performance measure of interest.

Table II – ANOVA Results for SR Study (p levels<.05\*)

Treatment Condition	Time off Target Trained Subjects	Time off Target All Subjects, All Runs
Chair Motion	p = 0.052 F = 9.747	p = .002* F = 20.546
Haptics	p = 0.019* F = 5.712	p = 0.028* F = 7.159
Chair Motion * Haptics (Interaction)	p = 0.579 F = .386	p = 0.415 F = 0.740

Since both haptics and task difficulty showed main effects but their interactions were not significant ( $p > .05$ ), it is concluded that we can reject the null hypothesis that tracking performance, using this dependent measure, was not significantly affected by the addition of the noise terms as previously described.

## DISCUSSION ON THE SR PERFORMANCE RESULTS

The data described in this report indicate that an optimal human interface design is possible with noise injected into the sensory modality system in two ways. With reference to Figure 9, it is observed that the minimum disturbance rejection error occurs when the stick noise is low and the chair noise is high. This represents an “optimal” human-machine interface design corresponding to the condition C1S1 in Figure 9. Thus a benefit has been gleaned by running the human operator within this scenario. The amount of improvement is indeed striking. Compared to the baseline condition (C0S0)

which would be the situation in a normal display, the optimum condition reduces the mean time off target error (across nine subjects) from 7.7 seconds to 3.34 seconds. This is a mean value of 56% reduction in time off target error for a disturbance rejection task. These results are significant, when averaged over the subject pool and in an operational environment, this can mean the difference between success and failure. Typically, in simulators, the COSO condition would represent an operator performing a remote mission in an UAV (unmanned air vehicle) system or in an on-orbit servicing task in a space operation scenario where the human has minimal situational awareness with the remote environment. The additional sensory modality information provided by the stick and the chair would assist in improving the awareness and performance level of the operator to perform this remote task. A discussion of the efficacy of the haptic stick to improve performance, situational awareness, and reduce workload has also been documented in Heath, et al., 2000 for the special application of UAV systems and operators working with tasks in remote locations with reduced alternative sensory modality information. It is now essential to discuss the issue of how the operator used his joystick controller when performing this disturbance rejection task when the human interface system is “optimally tuned”.

## **RESULTS FROM THE STICK AND CHAIR ORTHOGONALITY STUDY**

Since the human-machine interface system has been designed to optimize the interaction as depicted in Figure 9, this preeminent design configuration provides an opportunity to investigate characteristics of this interaction that may have been enhanced. In an earlier study (Repperger, 1991), it was demonstrated that when the force reflecting joystick had force characteristics that were *matched* to the “plant dynamics” under control, then two distinctiveness of this interaction were noted to occur:

- (1) The percent of stick (displacement) output of the joystick correlated with the target input forcing function  $f_T(t)$  was the highest when performance was most improved. This result was averaged over 5 pilot subjects and was a consistent measure (Repperger, 1991).
- (2) Also, the orthogonal component of the stick output to the target input forcing function  $f_T(t)$  was lowest when performance was most improved.

From an intuitive perspective, the results above seem plausible for several important reasons. First, when optimum tracking conditions occur, (minimum tracking error), the stick commands must be more useful in the sense they effectively track the target (have a higher component of correlation) in reducing the closed loop tracking error. Similarly, if the orthogonal component of the stick output is minimized, this implies the operator has focused his stick commands in a vector direction most productive to good tracking. Figure 11a illustrates this concept from a block diagram perspective, and Figure 11b is an adaptation of the data from the 1991 study where (using Fourier analysis) it was clearly demonstrated of the existence of this inverse relationship between tracking error and percent of stick output correlated with the target forcing function. It seems plausible that the same effects should have

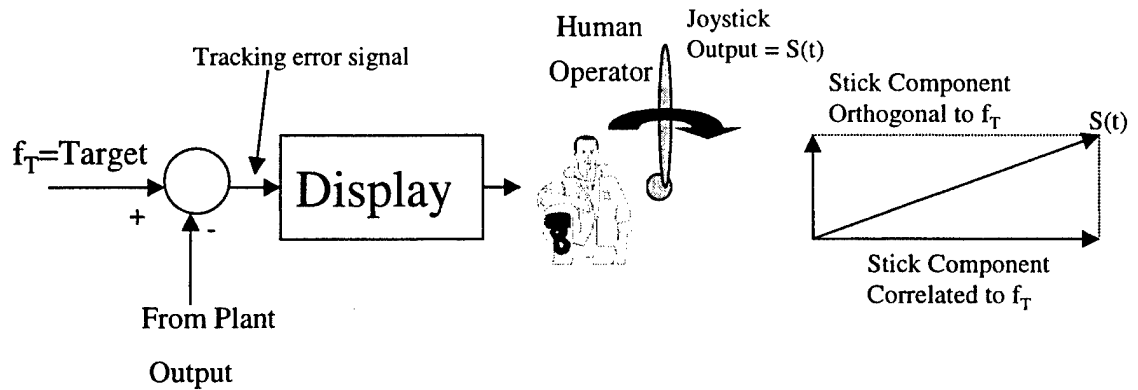


Figure 11a – Block Diagram Description Related to the Stick Orthogonality Issue

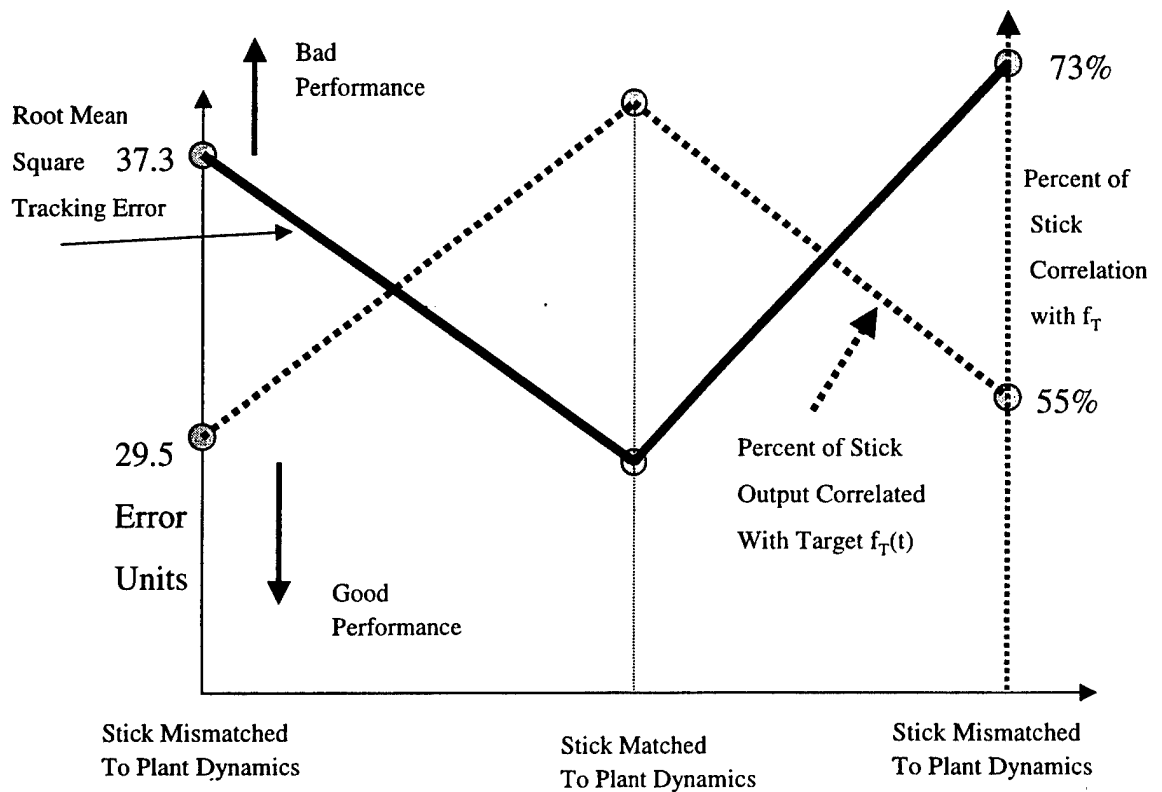


Figure 11b – Tracking Performance Results Dependent on The Stick Orthogonality Relationship

also appeared in the study described in this report if the human operator is operating as an efficient information processing system. To test this concept in the study discussed herein, the objective is first stated.

### Objective in Studying Orthogonal Stick and Chair Response

If the human operator is acting in an efficient manner during the “optimally tuned” machine-interface condition (C1S1 in Figure 9), then one would conclude that larger portions of the stick output commands from the operator are productive in the sense that they are more likely correlated with the target input forcing function. This may also be related to correlations of the chair motion. In terms of the null hypothesis we would like to reject.

### Hypothesis in Studying Orthogonal Stick or Chair Response

The null hypothesis we wish to reject is that when the operator is optimally tuned to the human-machine interface system, the percent of stick (or chair motion) output correlated to the target forcing function is not an important predictor of good tracking performance. Thus it is desired to reject:

*Ho:* The performance in the disturbance rejection task was not influenced or correlated with the stick or chair output.

### Data Analysis in Stick or Chair Orthogonality Study

For the stick and chair data orthogonality data analysis, first the stick motions made by the human will be analyzed. The target input forcing function was the sum of a

5 sine waves disturbance (quasi random in the sense it appears random to the human, but is truly a deterministic signal) which both moved the target  $f_T$  in a lateral direction and correspondingly could move the stick and/or the chair in the same lateral direction. The first analysis deals with the correlation between the stick output (a true command input from the human) with its coherency with the target tracking task using mean values across subjects. Figure 12a illustrates the relationship between performance (good performance is low amounts of time off target in a disturbance rejection task) and the correlation of the position displacement of the force reflecting controller in relation to the target tracking task. One may compare figure 12a with Figure 11b for the 1991 study with Air Force pilots. The mean values of these quantities are displayed when averaged over nine subjects for one day of data and the four experimental conditions of interest. It is noted that in Figure 12a, much like Figure 11b, that the experimental condition C1S1 gave rise to the optimum performance (minimum time off target) and highest percent of stick output correlated with the target.

To test this in a statistical context, SYSTAT<sup>®</sup> 8.0 was used to and Table III illustrates the significant effects from this ANOVA. In Table III, the p value and F values are given for the dependent performance measure of interest.

Table III – ANOVA Results for Stick and Chair Output Correlated with Target ( $p < .05^*$ )

Treatment Condition	Percent of Stick Output Correlated With Target	Percent of Chair Output Correlated with Target
Haptics (high or low)	$p = .005^*$ $F = 15.116$	$p = 0.186$ $F = 2.091$
Chair Motion (high or low)	$p = 0.337$ $F = 1.042$	$p < .001^*$ $F = 46.867$
Haptics * Chair Motion (Interaction)	$p = 0.413$ $F = 0.747$	$P = 0.381$ $F = 0.861$



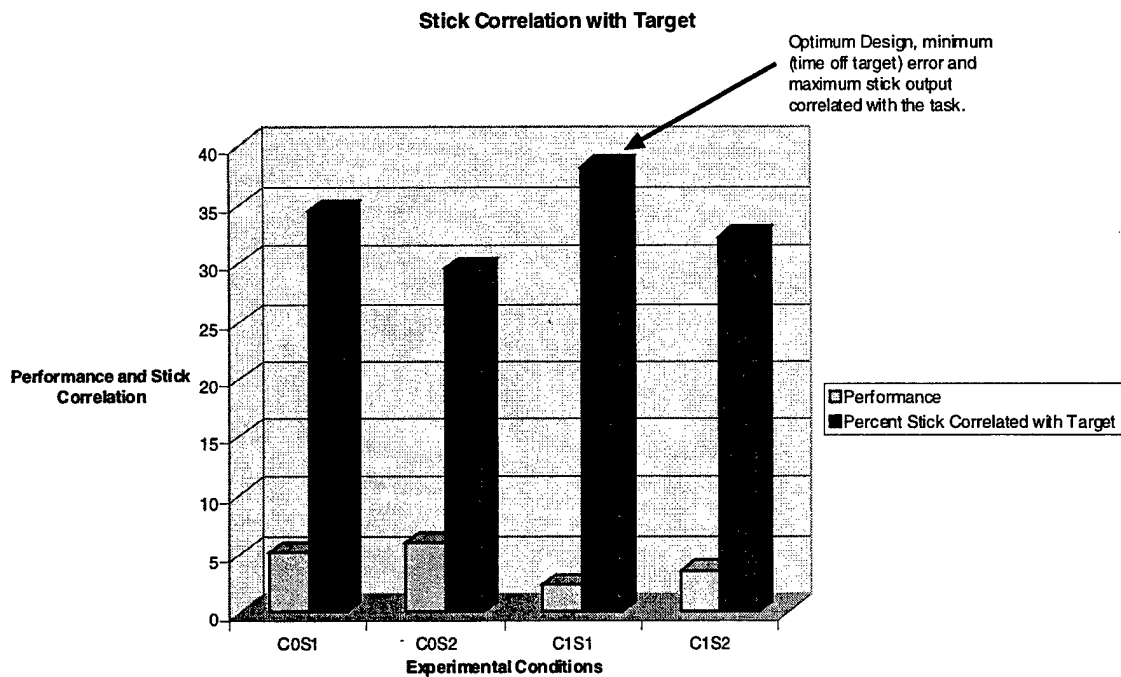


Figure 12a - Stick Correlation with Target Input- 9 Subjects Averaged

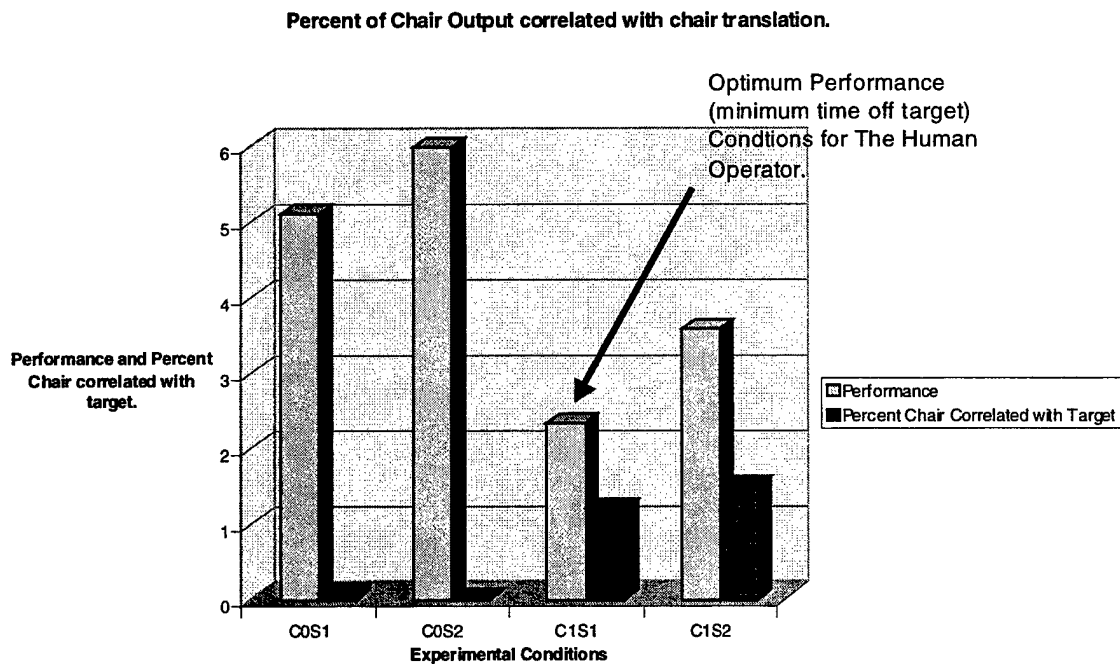


Figure 12 b - Chair Correlation with Target Input - 9 subjects averaged.

## **DISCUSSION OF THE STICK AND CHAIR ORTHOGONALITY STUDY**

As reflected in the mean values of the variables in Figures 12a-b, improved tacking performance was more related to high correlation of stick output with target but less pronounced with the high correlation of chair output with the target tracking signal. The statistical analysis portrayed in Table III reflected that in the cases where performance was enhanced (cf. Table II), the percent of stick output correlated with the target also was significantly different ( $p < .05^*$ ). In addition, when the chair motion made an impact on the tracking performance, both results were significantly different. Since both the haptics and the motion chair showed main effects, but their interactions were not significant ( $p < .05$ ), it is concluded that we can reject the null hypothesis that performance using these dependent measures (percent of correlation between two time signals), can be rejected at a 95% confidence level at least with respect to the stick output, which has no ambiguities.

## **CONCLUSIONS**

It has been demonstrated from a physics perspective, from a mathematical perspective, and also from an empirical validation that in certain situations, there may be some advantage in providing small amounts of noise stimulation into a human interface system. The injected noise is in the form of an alternative sensory modality (haptics and proprioceptive senses induced by a joystick and a motion chair device). The human operator is not unlike any other decision making system, which has to deal with uncertainties and other unknown task variables. The noise stimulation, when properly applied (using haptic and proprioceptive stimulation) can be designed in a judicious

manner to improve the operator's awareness of remote environments and to perform tasks where limited visual information is made available as well as in environments with reduced force feedback and other sensory modalities. This technique generalizes naturally to a host of different human-machine interactions in which fine-tuning of the interface may be enhanced by appropriate noise stimulation.

### *Acknowledgements*

The data analysis performed was supported, in part, by the AFOSR New World Vista Program, LRIR: 97AL007N11(NWV). The data analysis support was provided by R. Kinsler from Wright State University.

## **REFERENCES**

- Basso, M., Dahleh, M., Mezic, I. and Salapaka, M. V., "Stochastic Resonance in AFMs," *Proceedings of the American Control Conference*, San Diego, California, June, 1999, pp. 3774-3778.
- Benzi, R., Sutera, A., and Vulpiani, A., *Journal of Physics*, A14, L453-457, 1981.
- Bulsara, A. R., and Gammaitoni, L., "Tuning in to Noise," *Physics Today*, March, 1996, pp. 39-45.
- Chapeau-Blondeau, F., "Input-Output Gains for Signal in Noise in Stochastic Resonance," *Physics Letters A*, vol. 232, 21 July, 1997, pp. 41-48.
- Christini, D. J., and Collins, J. J., "Control of Chaos in Excitable Physiological Systems: A Geometric Analysis," *American Institute of Physics*, Vol. 7, No. 4, 1997, pp. 544-549.
- Collins, J. J., Chow, C. C., and Imhoff, T. T., "Stochastic Resonance Without Tuning," *Nature*, Vol. 376, 20 July, 1995a, pp. 236-238.
- Collins, J. J., Chow, C. C., and Imhoff, T. T., "Aperiodic Stochastic Resonance in Excitable Systems," *Physical Review E*, Vol. 52, No. 4, October, 1995b, pp. R3321-R3324.

Collins, J. J., Imhoff, T. T., and Grigg, P., "Noise-enhanced Tactile Sensation," *Nature*, Vol. 383, 31 October, 1996a, p 770.

Collins, J. J., Chow, C. C., Capela, A. C., and Imhoff, T. T., "Aperiodic Stochastic Resonance," *Physical Review E*, Vol. 54, No. 5, November, 1996b, pp. 5575-5584.

Collins, J. J., Imhoff, T. T., and Grigg, P., "Noise-mediated Enhancements and Decrements in Human Tactile Sensation," *Physical Review E*, Vol. 56, No. 1, July, 1997, pp. 923-926.

Cordo, P., Inglis, J. T., Verschueren, S., Collins, J. J., Merfeld, D. M., Rosenblum, S., Buckley, S., and Moss, F., "Noise in Human Muscle Spindles," *Nature*, Vol. 383, 31 October, 1996, pp. 769-770.

Fauve, S. and Heslot, F., *Physics Letters*, Vol. 97A, pp. 5-7, 1983.

Gailey, P. C., Neiman, A., Collins, J. J., and Moss, F., "Stochastic Resonance in Ensembles of Nondynamical Elements: The Role of Internal Noise," *Physical Review Letters*, Vol. 79, No. 23, 8 December, 1997, pp. 4701-4704.

Gammaitoni, L., Hanggi, P., Jung, P., and Marchesoni, F., "Stochastic Resonance," *Reviews of Modern Physics*, Vol. 70, No. 1, January, 1998, pp. 223-287.

Heath, R.A., Draper, Mark H., Lu, Liem G., Poole, Michael R., Repperger, Daniel W., "Haptic Feedback as a Supplemental Method of Alerting UAV Operators to the Onset of Turbulence," *Proceedings of the International Ergonomics Assn XIVth Triennial Congress and Human Factors and Ergonomics Society 44th Annual Meeting*, 30 Jul, 2000.

Heneghan, C., Chow, C. C., Collins, J. J., Imhoff, T.T., Lowen S. B., and Teich, M. C., "Information Measures Quantifying Aperiodic Stochastic Resonance," *Physical Review E*, Vol. 54, No. 3, September, 1996, pp. R2228-2231.

Loerincz, K., Gingl, Z., Kiss, L. B., "A Stochastic Resonator is Able to Greatly Improve Signal-to-Noise Ratio," *Physics Letters A*, Vol. 224, 30 December, 1996, pp. 63-67.

Longtin, A., "Stochastic Resonance in Neuron Models," *Journal of Statistical Physics*, Vol. 70, Nos. 1 and 2, 1993, pp. 309-327.

Martin, C. F. and Schovanec, L., "A Control Model of Eye Movement," *Proceedings of the 36<sup>th</sup> Conference on Decision and Control*, December, 1997, pp. 1135-1139.

McNamara, B. and Wiesenfeld, K., "Theory of Stochastic Resonance," *Physical Review A*, Vol. 39, No. 9, May 1, 1989, pp. 4854-4869.

Rajaram, R., Salapaka, M. V., Basso, M., and Dahleh, M., "Experimental Study of Stochastic Resonance in Atomic Force Microscopes," *Proceedings of the American Control Conference*, Chicago, Illinois, June 2000, pp. 2129-2133.

Repperger, D. W., Rogers, D. B. and Bianco, W. N., "Behavioral Modeling - Validation and Information Theory Considerations," International Journal of Mathematical Modeling, 4:209-222, 1983.

Repperger, D. W., "Active Force Reflection Devices in Teleoperation," *IEEE Control Systems Magazine*, January, 1991, pp. 52-56.

Repperger, D. W., Phillips, C. A. and Chelette, T., "Study of Spatially Induced 'Virtual Force' With An Information Theoretic Investigation of Human Performance," *IEEE Transactions on Systems, Man, and Cybernetics*, Vol. 25, No. 10, October, 1995, pp. 1392-1404.

Repperger, D. W., Haas, M. W., Brickman, B. J., Hettinger, L. J., Lu, L., and Moe, M., "Design of A Haptic Stick Interface as A Pilot's Assistant in A High Turbulence Task Environment," *Perceptual and Motor Skills*, vol. 85, 1997, pp. 1139-1154.

Richardson, K. A., Imhoff, T. T., Grigg, P., and Collins, J. J., "Encoding Chaos in Neural Spike Trains," *Physical Review Letters*, Vol. 80, No. 11, 16 March, 1998, pp. 2485-2488.

Strogatz, S. H., *Nonlinear Dynamics and Chaos*, Addison-Wesley Publishing Company, 1994.

Svirskis, G. and Rinzel, J., "Influence of Temporal Correlation of Synaptic Input on the Rate and Variability of Firing in Neurons," *Biophysics Journal*, August, 2000, Vol. 79, No. 2, pp. 629-637.

Wiesenfeld, K., and Moss, F., "Stochastic Resonance and the Benefits of Noise: from Ice Ages to Crayfish and Squids," *Nature*, Vol. 373, 5 January, 1995, pp. 33-36.

Wilson, H. R., "Simplified Dynamics of Human and Mammalian Neocortical Neurons," *J. Theoretical Biology*, Vol. 200, 1999, pp. 375-388.

Yang, Tao, "Adaptively Optimizing Stochastic Resonance in Visual Systems," *Physics Letters A*, Vol. 245, 1998, pp. 79-86.

Zames, G., and Shneydor, N. A., "Dither in Nonlinear Systems," *IEEE Transactions on Automatic Control*, Vol. AC-21, No. 5, October, 1976, pp. 660-667.

## APPENDIX A – Derivation of S/N Ratios for Linear Systems

Referring to Figure 13, it will be shown in this appendix that for a linear system, the addition of the noise term  $\xi(t)$  to a deterministic signal  $S(t)$  can only degrade the signal/noise ratio in the output variable  $y(t)$ . To show this result, we have for the output of the linear system the following representation:

$$Y(s) = H(s) [\bar{S}(s) + N(s)] \quad (\text{A.1})$$

where the Laplace transformation notation has been used and  $N(s)$  is the frequency equivalent of the power spectrum of the input noise process. The result in equation (A.1) holds due to the superposition property of the linear system displayed in Figure 13. The noise process  $N(s)$  may be white-gaussian or possibly a colored noise process. Since the input signal of interest  $S(t)$  is deterministic, we examine its spectral components by allowing  $s = j\omega$  in equation (A.1). Thus in the output signal  $Y(j\omega)$ , at each frequency  $\omega = \omega_s$ , the total power is due to power contributed by the deterministic signal  $\bar{S}(j\omega)$  as well as from the stochastic noise process  $N(j\omega)$ . Since:

$$Y(j\omega) = H(j\omega) [\bar{S}(j\omega) + N(j\omega)] \quad (\text{A.2})$$

then the ratio of signal to noise appearing in the output signal  $y(t)$  can be written:

$$\frac{Y}{Y_N} = \frac{[\bar{S}(j\omega) + N(j\omega)]}{N(j\omega)} \frac{H(j\omega)}{H(j\omega)} = 1 + \frac{\bar{S}(j\omega)}{N(j\omega)} \quad (\text{A.3})$$

To see the effect of increasing noise on this signal/noise ratio term in equation (A.3), Figure 14 illustrates a plot of  $y=1+1/x$  for positive values of  $x$  larger than zero. It is easy to show the decreasing monotonicity of this plot which, for increasing  $x$  from zero, means if both  $\alpha > 0$  and  $\beta > 0$  with  $\alpha > \beta$ , then it is strictly true that  $y(\alpha) < y(\beta)$ .

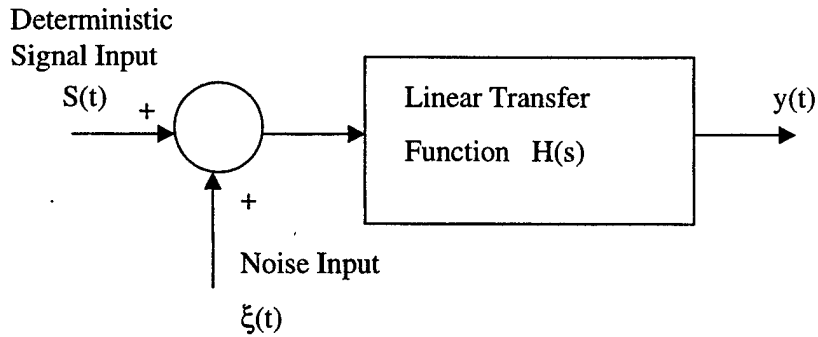


Figure 13 – SR in A Linear System

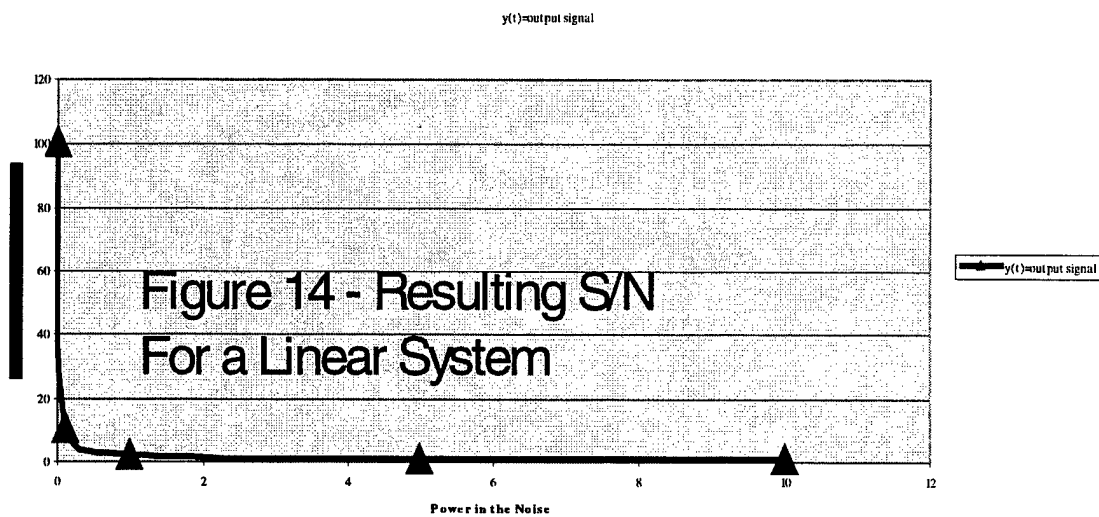


Figure 14 – Resulting S/N for a Linear System

## APPENDIX B – Derivation of S/N Ratio for Certain Nonlinear Systems

This appendix will illustrate an effect which is not demonstrated in Appendix A, i.e. where the stochastic disturbance, when added to a nonlinear system, can be shown to improve certain transfer characteristics of some important variables. The results presented here will follow Chapeau-Blondeau, 1997 with some remarks made from a very interesting result demonstrated by Loerincz, et al. 1996. In this notation, the following variables will be used:

Let  $S(t)$  = a coherent, periodic, signal of period  $T_s$ .

Let  $\xi(t)$  = a stationary white noise.

The white noise term  $\xi(t)$  has probability density function  $f_\eta(u)$  which is assumed to be normal and Gaussian. The distribution function of the random variable  $\xi(t)$  is specified via:

$$F_\eta(u) = \int_{-\infty}^u f_\eta(u') du' \quad (B.1)$$

The nonlinear operator of Figure 15 is specified by  $g(\cdot)$ . Hence the output  $y(t)$  is of the form:

$$y(t) = g[S(t) + \xi(t)] \quad (B.2)$$

Thus the coherent part of  $y(t)$  shows up in the output power spectral density as spectral lines at integer multiples of the coherent frequency  $1/T_s$ . The power contained in the coherent spectral line at frequency  $\frac{n}{T_s}$  is given by  $|\bar{Y}_n|^2$  where  $\bar{Y}_n$  is the  $n$ th order Fourier coefficient of the  $T_s$  – periodic nonstationary output mean  $E\{y(t)\}$  where:

$$\bar{Y}_n = \frac{1}{T_s} \int_0^{T_s} E\{y(t)\} e^{[-i(n\frac{2\pi}{T_s})t]} dt \quad (B.3)$$



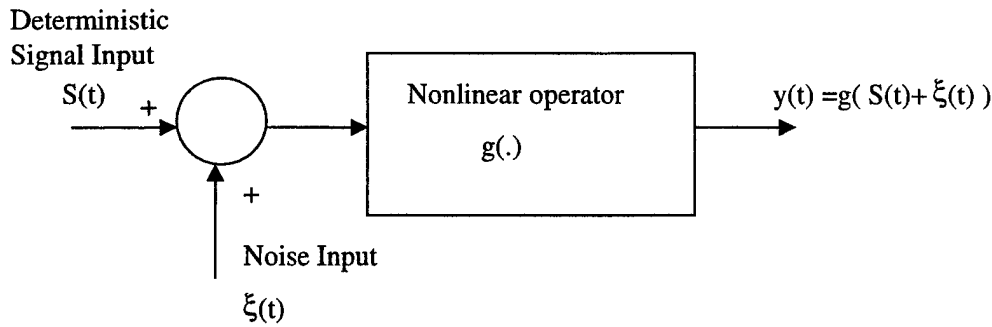


Figure 15 – SR in A Nonlinear System

which implies  $\omega = \frac{2\pi}{T_s} n$  is the  $n$ th coherent frequency. This is well known, for example, from signal processing theory, that the Fourier transform  $F(\omega)$  of a time signal  $f(t)$  can be specified via:

$$F(\omega) = \int_{-\infty}^{\infty} f(t) e^{-j\omega t} dt \quad (\text{B.4})$$

Since  $g(\cdot)$  is a static nonlinearity, the first and second moments of  $y(t)$  which operate on  $g(\cdot)$  are calculated. It is necessary to realize that we are dealing with an output of a nonlinear system, consequently certain superposition properties may not hold. For the first moment, the mean of the possibly nonstationary variable  $E\{y(t)\}$  can be computed at time  $t$  from the classical definition of the first moment or mean of a variable, which is specified via:

$$E\{y(t)\} = \int_{-\infty}^{\infty} g(u) f_{\eta}[u - S(t)] du \quad (\text{B.5})$$

where the density function  $f_{\eta}(u')$  is modified to account for the real time additivity between the deterministic signal  $S(t)$  and the noise source  $\xi(t)$ . To compute the second moment of  $y(t)$ , first denote (for a random variable  $x(t)$ ) with mean:

$$\bar{x} = E\{x\} = \int_{-\infty}^{\infty} x f(x) dx \quad (\text{B.6})$$

where  $f(x)$  symbolizes the density function of the random variable  $x(t)$ . The second moment  $\sigma$  or variance of  $x(t)$  can be written (for the random variable  $x(t)$ ), in general, as:

$$\sigma^2 = E\{(x - \bar{x})^2\} = \int_{-\infty}^{\infty} (x - \bar{x})^2 f(x) dx \quad (\text{B.7})$$

or:

$$\sigma^2 = E\{x^2\} - [E\{x\}]^2 = E\{x^2\} - \bar{x}^2 \quad (\text{B.8})$$

When applying equations (B.7 – B.8) to the output variable  $y(t)$ , the second moment becomes:

$$\text{var}[y(t)] = \int_{-\infty}^{\infty} g^2(u) f_{\eta}[u - S(t)] du - \left( \int_{-\infty}^{\infty} g(u) f_{\eta}(u - S(t)) du \right)^2 \quad (\text{B.9})$$

Since this is a stochastic process, we define the mean value of the variance of  $y(t)$  over one period  $T_s$  via:

$$\overline{\text{var}(y)} = \frac{1}{T_s} \int_0^{T_s} \text{var}[y(t)] dt \quad (\text{B.10})$$

where  $\text{var}[y(t)]$  is characterized in (B.9). For the overall input  $S(t) + \xi(t)$ , the coherent

component is measured by the spectral line at the frequency  $\frac{n}{T_s}$ . The coherent power is

specified via  $|S_n|^2$  via the order  $n$  Fourier coefficient of  $S(t)$  as follows:

$$S_n = \frac{1}{T_s} \int_0^{T_s} S(t) e^{-i(\frac{n2\pi}{T_s} t)} dt \quad (B.11)$$

To determine the transfer characteristics it is necessary to examine the output/input at the coherent spectral lines. For the deterministic signal term, the transfer characteristics are specified via:

$$G_{sig}(\frac{n}{T_s}) = \frac{|\bar{Y}_n|}{|S_n|} \quad (B.12)$$

It is necessary to normalize with respect to the two variances including the input white noise variance  $\sigma_n$  as well as the deterministic signal. At the frequency  $\frac{n}{T_s}$  for the noise term it is seen that:

$$G_{noise} = \frac{\sqrt{\text{var}(y)}}{\sigma_n} \quad (B.13)$$

The overall signal to noise ratio can now be specified by:

$$G_{SNR}(\frac{n}{T_s}) = \frac{G_{sig}^2(\frac{n}{T_s})}{G_{noise}^2(\frac{n}{T_s})} = \frac{|\bar{Y}_n|^2 / \text{var}(y)}{|S_n|^2 / \sigma_n^2} \quad (B.14)$$

Thus the expression in equation (B.14) must be calculated for each input signal (and its respective density) as well as by the specific nonlinearity that is operated upon by the output vector  $y(t)$ . It is now desired to examine the hard nonlinearity of a threshold which is of interest in the use of stochastic resonance systems as discussed herein.

#### **The Particular Case of A Hard Nonlinearity $g(\cdot)$ Representing a Threshold:**

For a hard threshold, for an input  $u$ , the output  $y = g(u)$  satisfies (for threshold  $\theta$ ):

$$g(u) = 0 \quad \text{if } u < \theta \quad (B.15a)$$

$$g(u) = A_y \quad \text{if } u \geq \theta \quad (B.15b)$$

Using the relationships specified in equations (B.15a-b), they are substituted into (B.5) and (B.9) resulting in the following expressions for this particular nonlinearity:

$$E\{y(t)\} = A_y [ 1 - F_\eta(\theta - S(t)) ] \quad (B.16)$$

and 
$$\text{var}[y(t)] = A_y^2 F_\eta[\theta - S(t)] [1 - F_\eta(\theta - S(t))] \quad (B.17)$$

The second part of this procedure is to stipulate, very specifically, the type of input signal and its characteristics. For this simple example, the choice is made of  $S(t)$  being a train of square pulses of amplitude  $A_s > 0$  of time duration  $T$  seconds. This can be denoted as:

$$S(t) = A_s \quad \text{for } t \in [0, T] \quad (B.18a)$$

$$S(t) = 0 \quad \text{for } t \in [T, T_s] \quad (B.18b)$$

And the process is periodic every  $T_s$  seconds, repeating the above sequence of pulses. For the time series specified in equations (B.18a-b), the Fourier coefficients are given by:

$$S_n = A_s \frac{T}{T_s} \left[ \text{sinc}(n\pi \frac{T}{T_s}) e^{(-in\pi \frac{T}{T_s})} \right] \quad (B.19)$$

where the notation  $\text{sinc}(u) = \frac{\sin(u)}{u}$  is used. This results in the following complex

expressions for the first and second moments of the  $y(t)$  output variable of interest:

$$\bar{Y}_n = A_y \frac{T}{T_s} [F_\eta(\theta) - F_\eta(\theta - A_s)] \text{sinc}(\pi n \frac{T}{T_s}) e^{(-in\pi \frac{T}{T_s})} \quad (B.20)$$

and 
$$\overline{\text{var}}(y) = A_y^2 \left\{ \left[ \frac{T}{T_s} F_\eta(\theta - A_s) \right] [1 - F_\eta(\theta - A_s)] + \left(1 - \frac{T}{T_s}\right) F_\eta(\theta) [1 - F_\eta(\theta)] \right\} \quad (B.21)$$

This gives rise to the following expressions for the gain at the signal and noise component of  $y(t)$ :

$$G_{sig}(\frac{n}{T_s}) = \frac{A_y}{A_s} [F_\eta(\theta) - F_\eta(\theta - A_s)] \quad (B.22)$$

and:

$$G_{noise}(\frac{n}{T_s}) = \frac{A_y}{\sigma_\eta} \left[ \frac{T}{T_s} F_\eta(\theta - A_s) \{1 - F_\eta(\theta - A_s)\} + (1 - \frac{T}{T_s}) F_\eta(\theta) [1 - F_\eta(\theta)] \right]^{\frac{1}{2}} \quad (B.23)$$

Thus the overall signal to noise gain becomes:

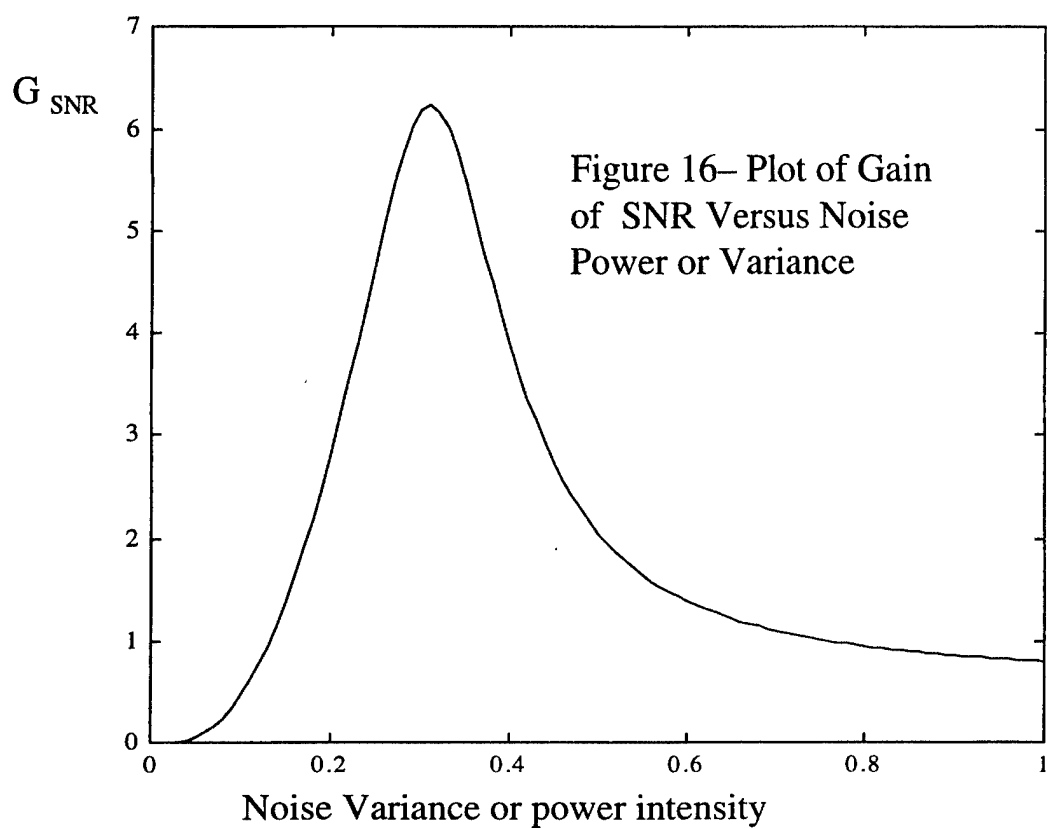
$$G_{SNR}(\frac{n}{T_s}) = \frac{\sigma_\eta^2}{A_s^2} [F_\eta(\theta) - F_\eta(\theta - A_s)]^2 \left\{ \frac{T}{T_s} F_\eta(\theta - A_s) [1 - F_\eta(\theta - A_s)] + (1 - \frac{T}{T_s}) F_\eta(\theta) [1 - F_\eta(\theta)] \right\}^{-1} \quad (B.24)$$

Now the presumption was that the input noise process is zero-mean Gaussian, hence it is characterized by the distribution function:

$$F_\eta(u) = \frac{1}{2} \left[ 1 + \operatorname{erf} \left( \frac{u}{\sqrt{2} \sigma_\eta} \right) \right] \quad (B.25)$$

Where: 
$$\operatorname{erf}(u) = 2 \int_0^u \exp(-u'^2) du' / \sqrt{\pi} \quad (B.26)$$

And Figure 16 portrays a simulation of the signal gain versus the noise RMS amplitude for the special case of parameters  $\theta = 1$ ,  $A_y = 1$  for the noise and threshold process. For the deterministic input  $S(t)$  the parameters were selected to be of the form  $T = 10^{-2} T_s$  and  $A_s = 0.97$ .



Finally, it is noted in Loerincz et al., 1996, that  $G_{SNR}$  may exceed 1.0 for special input sequences  $S(t)$  with certain density functions as is displayed in Figure 16.

## Appendix C – The Class of Systems That Exhibit SR

To examine what type of systems may exhibit the effect of stochastic resonance, a few preliminaries are in order (Strogatz, 1994). This analysis will be conducted from an energy perspective and it will be useful to visualize the dynamics of a nonlinear system based upon potential energy. Let  $V(x)$  denote the potential energy of a nonlinear system (and  $f(x)$  is the force) which is required to be specified via:

$$\dot{x}(t) = f(x) = -\frac{dV}{dx} \quad (C.1)$$

Hence the systems under consideration (for simplicity) will be nonhomogenous and of the autonomous type, i.e.  $f(x)$  depends only on  $x$  and not on the time variable  $t$ . There are physical reasons why the representation in equation (C.1) is chosen. From physics, force is the negative gradient of potential energy and thus equation (C.1) represents a physical system with  $V$  in the role of the potential energy function and  $f(x)$  representing a force vector. To make the system physically realizable, motion is produced on a particle sliding down the walls of a potential well (characterized by the potential energy function). Thus as the particle moves “downhill,” the motion proceeds. As the particle moves, it tries to achieve a lower potential energy (hence  $V$  is decreasing as we ride down the negative gradient). From the chain rule, the time derivative of  $V(x)$  can be written:

$$\frac{dV}{dt} = \frac{dV}{dx} \frac{dx}{dt} \quad (C.2)$$

But we chose only those nonlinear systems constrained to be of the form (of (C.1) i.e.):

$$\frac{dx}{dt} = -\frac{dV}{dx} \quad (C.3)$$

because of the relationship mandated in equation (C.1). Hence it follows from (C.2) that:

$$\frac{dV}{dt} = \left[ \frac{dV}{dx} \right] \left[ -\frac{dx}{dt} \right] = -\left( \frac{dV}{dx} \right)^2 \leq 0 \quad (C.4)$$

Thus  $V(x)$  decreases along motion trajectories and the particle moves toward a lower potential energy. At an equilibrium point (fixed point), then  $\frac{dV}{dx} = 0$  and  $V$  remains constant. This is also verified by the fact that:

$$\frac{dV}{dx} = -\dot{x} = 0 \quad (C.5)$$

is also a definition of an equilibrium (fixed point) since  $\dot{x} = 0$  is now satisfied in equation (C.5). Thus a local minimum of  $V(x)$  corresponds to a stable fixed point while a local maximum of  $V(x)$  corresponds to an unstable fixed point. Also from nonlinear dynamics (Strogatz, 1994), the fixed points must oscillate between stable and unstable equilibriums in a phase plane representation (assuming real fixed points), otherwise chaos will occur. The following example illustrates how to use results presented in the analysis so far.

### **Example:**

Consider the system: 
$$\dot{x} = x - x^3 = -\frac{dV}{dx} \quad (C.6)$$

To find the  $V(x)$  function, the first integral (with respect to  $x$ ) of:

$$\frac{dV}{dx} = -[x - x^3] \quad (C.7)$$

yields:

$$V(x) = -\frac{1}{2} x^2 + \frac{1}{4} x^4 + C \quad (C.8)$$

First we set  $C=0$  and find (by setting the right hand side of (C.6) to zero to find the equilibrium points) that a local minimum of  $V(x)$  exists at  $x = \pm 1$  and a local maximum exists at  $x = 0$ . Since the local minima are separated by a local maximum, this system can demonstrate stochastic resonance. This is a double-well potential surface and the system



is said to be bistable since it has two stable equilibria (separated by an unstable equilibrium point). Figure 17 for  $V(x)$  and Figure 18 illustrate the fixed points of this example (cf. Figures 2-3).

To show a linear system can never exhibit stochastic resonance, start first with:

$$-\frac{dV}{dx} = f(x) = \dot{x} \quad (C.9)$$

If  $f(x)$  were linear in  $x$ , then  $V(x)$  (the first spatial integral of (C.9)) would be of the order of  $O(x^2)$ , at worst. Taking the first derivative of  $V(x)$  and setting it to zero would yield only one maximum or minimum. Hence, there exists only one fixed point for a linear system. From Figures 17-18, it is known that at least three fixed points are required with a local maximum occurring between two local minimums in order for stochastic resonance to transpire. From this discussion, the following rules can be gleaned for the type of nonlinear systems that would exhibit stochastic resonance:

Rules for nonlinear systems to exhibit stochastic resonance ( $\dot{x} = f(x)$ ):

- (1)  $f(x)$  must have powers  $x$  of 3 or higher (at least 3 fixed points must occur).
- (2) The fixed points resulting from setting  $f(x)=0$  must have two local minimums (stable fixed points) separated by a local maximum (an unstable fixed point).

Note there are an infinite class of systems that satisfy the above two conditions and  $f(x)$  may contain higher powers of  $x$  but the fixed points must be interlaced and alternated between stable and unstable equilibriums. Some additional systems are now listed that also exhibit SR effects, which are synthesized, based on the above discussion.

$$\dot{x} = (x+1) [2+x] [2-x] \quad (C-10)$$

$$\dot{x} = (x+2) [4+x] [4-x] [10+x][10-x] \quad (C-11)$$

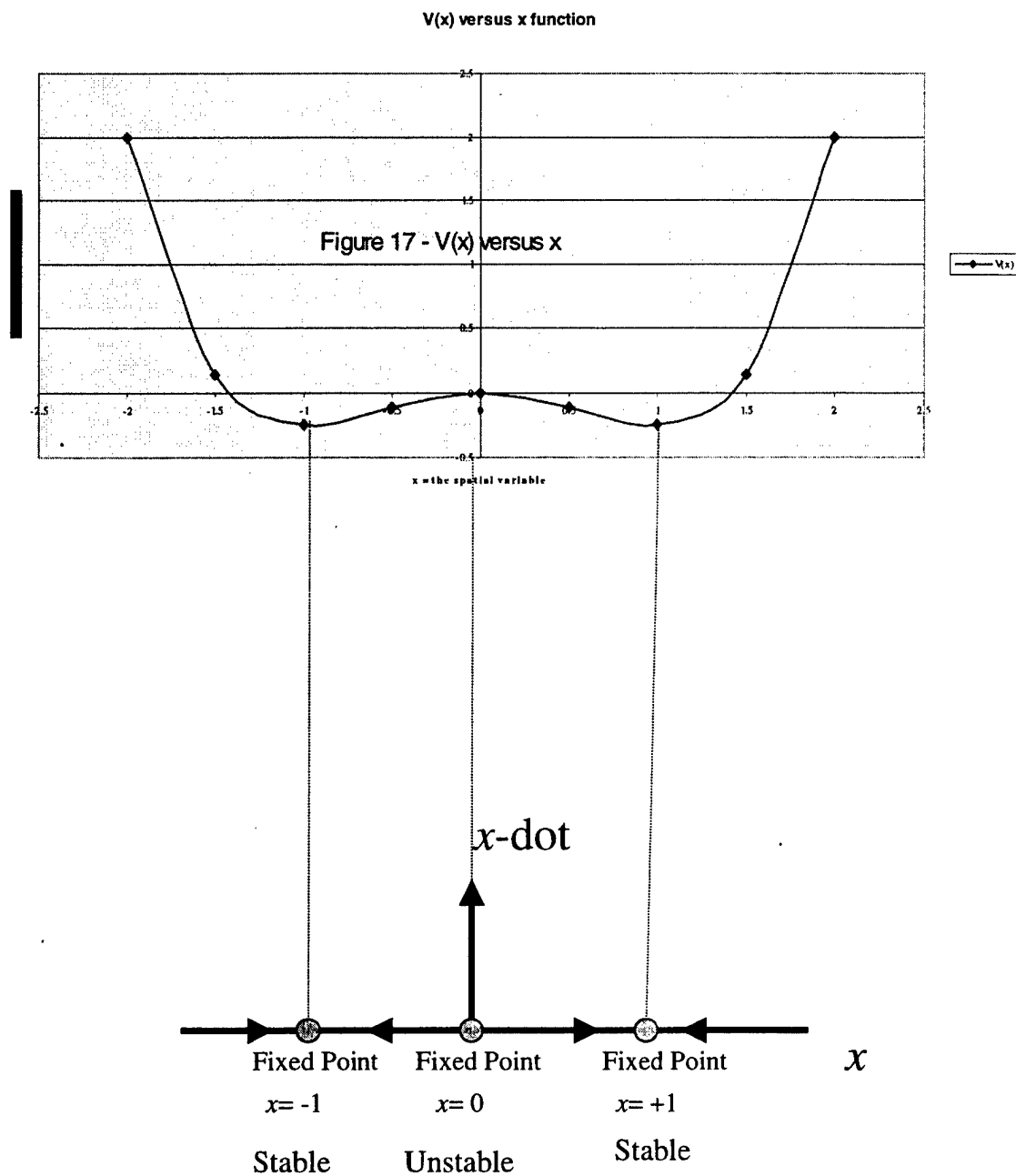


Figure 18– Fixed Points for Figure 17

$$\dot{x} = (x+4) [6+x] [6-x] [8+x][8-x][10+x][10-x] \quad (\text{C-12})$$

etc. Thus a method is given to synthesize nonlinear systems so that SR occurs.